Food & Function

Accepted Manuscript

ROYAL SOCIETY OF CHEMISTRY

rsc.li/food-function

View Article Online
DOI: 10.1039/C7FO01239J

Effect of anthocyanins from red wine and blackberry on the integrity of a keratinocyte model using ECIS

Ana Évora[†]
Victor de Freitas[†]
Nuno Mateus[†]
Iva Fernandes*[†]

[†]REQUIMTE/LAQV, Department of Chemistry and Biochemistry, Faculty of Sciences, University of Porto, Porto, Portugal.

*E-mail: iva.fernandes@fc.up.pt; Tel: +351.220402562

View Article Online
DOI: 10.1039/C7FO01239J

Abstract

There is a growing market demand for the incorporation of plant-derived ingredients in new products for the cosmetic industry. Anthocyanins are polyphenols arising from plant secondary metabolism that have been shown to display many bioactive properties such as free radical scavenging, antimicrobial, and chemopreventive activities. In this work, the biological activities of red wine and blackberry anthocyanins were assessed by developing a new keratinocyte barrier model using HaCat cell line and a microelectrode-based biosensor device, referred to as Electric Cell-Substrate Impedance Sensing (ECIS). Cells were seeded at the optimal cellular density of 1.6 x 10^6 cells/mL and the half-time was calculated to be 3.55 ± 0.67 hours. Compounds' cytotoxicity was assessed and anthocyanin pigments showed no cytotoxicity towards keratinocyte cells. Wound healing assays were also performed using ECIS and it was observed that the tested pigments enhanced the healing rate of keratinocyte cells by reducing the healing time more than 50 %. Cyanidin-3-glucoside presented the best results recovering 50 % of the injured area in 1.48 (± 0.15) hours, followed by the blackberry anthocyanins (2.01 ± 0.18 hours), malvidin-3-glucoside (2.03 ± 0.09 hours) and red wine anthocyanins (2.36 ± 0.76 hours). All presented significant differences from the control 4.91 (± 1.11) hours.

Abbreviations

Dp3glc: delphinidin-3-O-glucoside; Pt3glc: petunidin-3-O-glucoside; Pn3glc: peonidin-3-O-glucoside; Mv3glc: malvidin-3-O-glucoside; Cy3glc: Cyanidin-3-O-glucoside; Cy3rut: Cyanidin-3-rutinoside, Cy3dioxaglc: Cyanidin-3-dioxaloyl-glucoside, Cy3manglc: Cyanidin-3-malonyl-glucoside.

1. Introduction

View Article Online
DOI: 10.1039/C7FO01239J

Plant metabolites are gaining popularity as cosmetic ingredients for being natural compounds and possessing many biological activities [1]. Phenolic compounds are secondary plant metabolites, produced in response to several stimuli, such as ultraviolet radiation, wounding and infections. These phenolic compounds could be applied in skincare products, to prevent external skin damage. Among those are anthocyanins, phenolic compounds belonging to the flavonoid subclass, and responsible for the cyanic colours of most fruits and flowers of angiosperms. They have been shown capable of inhibiting tumor growth and reducing inflammation, but also to have antimicrobial, metal-chelating and free radical scavenging activities [2, 3]. They are usually used in the food industry [4] as natural colorants and antioxidants, but their ability to prevent oxidative damages make them potential novel compounds for cosmetic formulations, as they may prevent skin diseases and premature aging[5].

Skin is the largest and most important protective barrier that blocks the entry of foreign pathogens into the body. At the same time, it protects internal organs from mechanical and UV irradiation damages, and it also helps in the regulation of body temperature and in the loss of fluids [6]. As skin is the first barrier against external assaults, it is more susceptible to the occurrence of wounds. Wound healing is a complex process composed of four phases involving self-repair of tissue after various injuries [7]. When a wound is formed, keratinocytes and fibroblasts migrate and proliferate to the wounding site [6]. Gap closure is observed microscopically over time as cells move and proliferate to fill the damage area and so, wound-healing assays, such as the scratch assay, the cell-exclusion zone assay and others, have been used to estimate migration and proliferation rates [7]. However, these are usually non-reproducible and time-consuming assays.

This phenomenon can then be monitored in real-time using the electric cell-substrate impedance sensing (ECIS) technique, which relates the changes in impedance measurements with cellular behaviour [8]. The ECIS device monitors the impedance of small gold-coated electrodes used as support for cells in culture and can be used to detect subtle changes in the cell-matrix interaction [8]. This device was first used by Giaever and Keese in 1991 [9] and since then several users have been able to explore its versatility in studying different cellular phenomena such as the cell attachment and spreading [10], cell motility [11], barrier function of cell layers [12], and in vitro toxicology [13-15]. A commonly used assay for cytotoxicity using this system takes the time course of overall impedance of a cell-covered electrode after the addition of compounds and

View Article Online
DOI: 10.1039/C7FO01239J

estimates the half-inhibition concentration [15]. However, the small fluctuations in impedance, normally associated with living cells, can be measured and analysed to understand the effect of compounds on cellular motion [13].

Wound-healing assays in ECIS are performed by applying a high electrical current to a confluent cell monolayer, creating an empty space on the surface of the electrode. The healing process is then monitored continuously, measuring impedance over time. These measures reflect the migration and proliferation of cells from the microelectrode surroundings to its surface [16].

Bearing this, in this work, the optimization of a new keratinocyte monolayer model using a microelectrode-based biosensor device, ECIS, is described and the effect of anthocyanins on wound healing process is explored.

2. MATERIALS AND METHODS

2.1 Reagents

Fetal bovine serum (FBS), 0.25 % trypsin-EDTA, trypan blue, PBS, pyruvic acid, sulforhodamine B (SRB), tris-HCl, and antibiotic/antimycotic solution (100 x), DMEM-F12 and RPMI media were purchased from Sigma-Aldrich (Madrid, Spain). Acetic glacial acid and dimethyl sulfoxide (DMSO) were purchased from Fluka (Madrid, Spain). Trichloacetic acid (TCA) was purchased from Merck (Darmstadt, Germany). Tissue culture supports were supplied by TPP (Trasadingen, Switzerland).

2.2 Anthocyanin Extraction and Purification

Anthocyanins were extracted from wine and blackberries. The preparation of wine anthocyanins extract was performed as described elsewhere with minor changes [17]. Red wine anthocyanin rich extract was obtained from the concentration of 50 litres of red wine in a nanofiltration system followed by the evaporation of ethanol. Sugars were removed by C18 reverse gel column chromatography. This crude extract was freeze-dried. An extraction with ethyl acetate was performed to remove non-anthocyanin organic compounds from 5 g of the lipophilized red wine. The aqueous layer was then applied in a Büchner funnel loaded with C18 reverse gel and the anthocyanin 3-monoglucosides were eluted with 30 % methanol acidified with HCl 0.01 %. Methanol was removed by evaporation. The aqueous phase was concentrated and freeze-dried. For the purification of malvidin-3-glucoside, 20 mg of the red wine anthocyanin extract

View Article Online
DOI: 10.1039/C7FO01239J

was applied to a C18 reverse gel column and Mv3glc was eluted with 20 % methanol acidified with HCl 0.01 %.

An extract rich in anthocyanins from blackberry was obtained from 1 kg of fresh blackberries. Extraction was performed with 5 litres of 50 % methanol acidified with HCl 0.01 % for 2 hours, after which solvent was changed for new one and extraction was allowed for more 24 hours. Methanol was evaporated and the aqueous phase was applied to a Büchner funnel loaded with C18 reverse gel to remove sugars. Elution of total anthocyanins was done with 50 % methanol acidified with HCl 0.01 %. For the purification of Cy3glc, the same process was followed, but elution form C18 reverse gel was performed with 10 % methanol for isolation of Cy3glc.

2.3 HPLC

Anthocyanins from wine and blackberry extracts were analysed as described elsewhere [17, 18]. Purity degree of the isolated Mv3glc and Cy3glc were estimated by injection on Elite Lachrom system (L-2130) equipped with a reversed-phase C18 (Merck, Darmstadt) (250 × 4.6 mm i.d.). Solvents were (A) water/formic acid 9:1 (v:v) and (B) acetonitrile, with the following gradient: 10-35 % B over 50 min at a flow rate of 0.5 mL/min.

2.4 Cell Culture

An aneuploid immortal keratinocyte cell line from adult human skin, HaCat, was grown as a monolayer from passage number 35 to 55. For routine maintenance, cells were cultured in 25 cm^2 monolayer in DMEM-F12 or RPMI (Sigma, Madrid, Spain) medium supplemented with 10% heat-inactivated FBS and 1% antibiotic/antimycotic solution (100 units mL^{-1} of penicillin, 100 µg mL^{-1} of streptomycin and 0.25 µg mL^{-1} of amphotericin B) at 37 ºC in a humified atmosphere with 5% CO_2. Cells were harvested by trypsinization (0.25% (w/v) trypsin-$EDTA_4Na$) twice a week.

2.5 Sulforhodamine B Assay

The effect of anthocyanin extracts and their major isolated anthocyanins on the growth of the human keratinocyte cell line (HaCat) was assessed according to the procedure adopted by the US National Cancer Institute in the '*'In vitro Anticancer Drug Discovery Screen''* that uses the protein-binding dye SRB to assess cell growth. HaCat cells were first grown into 96-well plates at a cellular density of 1.5×10^5 cell/mL in

View Article Online
DOI: 10.1039/C7FO01239J

RPMI (Sigma, St. Louis, MO) medium and allowed to grow for 24 hours. Thereafter, cells were incubated with a five-serial concentration of the extracts/compounds (6.3, 12.5, 25, 50 and 100 μM), for 48 hours, with a maximal solvent concentration (DMSO) of 0.05%. TCA (50% solution) was then added and after 1h at 4ºC, the plates were washed four times with deionized water and allowed to dry overnight. The wells were then stained with 0.4% solution of SRB for 30 min in the dark. The excess of staining solution was washed out with 1% acetic acid. The bound stain was solubilized with tris-buffer (10 mM, pH 8.0) and absorbance was measured at 492 nm in a microplate reader (Powerwave XS, Bio-Tek Instruments Inc.). Cytotoxicity was determined as percent survival, calculated by the number of treated (*T*) over the control (*C*) cells × 100% (% *T/C*).

2.6 Electric Cell-Substrate Impedance Sensing (ECIS) Assay

A commercial ECIS system (Applied Biophysics, Troy, NY, USA) was employed to measure the impedance associated with the proliferation of human keratinocyte cells. The ECIS system can simultaneously measure cell resistance and capacitance during cell culture. 8W1E sensing chips consisting of eight separate wells which were 1 cm in height and 0.8 cm^2 cm in bottom area were used. One detecting electrode of 250 μm in diameter is deposited on the bottom of each well and connected in series to a 1 MΩ resistor, an AC signal generator and a large gold counter electrode. Since the AC signal amplitude is set to 1 V, it results in a current source with the amplitude of 1 μA. The in-phase voltage was proportional to the resistance and the out-of-phase voltage was proportional to the capacitive reactance.

2.6.1 Keratinocyte Monolayer Model Optimization Using ECIS

A pre-treatment of the electrodes was performed as described in literature [8]. 8W1E PET electrodes were used as they are ideal for wound healing assays. They were first treated with 10 mM L-cysteine solution for 15 min, for cleaning and to improve well-to-well reproducibility and signal-to-noise ration Wells were washed 3 times with sterile ultrapure water and incubated with 1% gelatin solution for 30 min. After washing, 500 μL of DMEM-F12 medium were added to each well to check resistance and capacitance basal values. If the cleaning process was successful (basal resistance values around 2000 Ω and capacitance around 5 nF), cells were inoculated at two different cellular densities (1.6×10^5 or 1.6×10^6 cells/mL) with DMEM-F12, in a final volume of 500

View Article Online
DOI: 10.1039/C7FO01239J

μL. Cells were allowed to attach to the electrodes outside the incubator for 30 min. After 24 hours in culture, the confluency and viability of the cell monolayer was confirmed by light microscopy and electrically by impedance measurements. Half or total medium was renewed 20 h after inoculation and cells were allowed to adapt for 4 hours. Thereafter, 250 μL of compound solutions were applied to each well at a final concentration of 20 μM and the arrays were incubated for 24 hours. A positive control with DMSO was performed to validate cytotoxicity assays. DMSO was the solvent in which stock solutions were prepared. 4 replicates were made for each DMSO concentration (0.05%, 1%, 5% and 10%). The electrical impedance of each well was measured every 2 min and up to 16 individual wells were followed successively.

Cytotoxicity was assessed by taking impedance measures and applying the mathematical model developed by Giaever and Keese [9]. It can be used to calculate morphological parameters, as the barrier function of the cell layer, the spacing between the ventral side of the cell and the substratum, and the cell membrane capacitance. Cell micromotion analysis was also performed as a measure of cytotoxicity. Impedance data were taken every second until 2048 points were acquired for each well, in sequence. Noise data was normalized and analysed by means of FFT transform, variance (the square of the standard deviation) and the variance of increments as previously described [11].

2.6.2 ECIS Wound Assay

Wound-healing assays were performed after incubation of HaCat cells with compounds for 24 hours. Wounding was performed by applying an AC current of 2400 μA, 60 kHz for 60 s, killing the cells on the surface of the electrode which resulted in an abrupt drop in impedance to values like those of a cell-free electrode. Healing process was monitored continuously as cells migrated and proliferated onto the electrode.

2.7 Stastical Analysis

Statistical significance of the difference between various groups was evaluated by one-way analysis of variance (ANOVA), followed by the Bonferroni test. Differences were statistically significant when $*p < 0.05$ vs control.

3. RESULTS AND DISCUSSION

View Article Online
DOI: 10.1039/C7FO01239J

The red wine anthocyanin rich extract was analysed and confirmed that malvidin-3-glucoside (4, Mv3glc) represents the main anthocyanin present (Figure I.A). The other minor peaks correspond to the following anthocyanins: 1, delphinidin-3-glucoside (Dp3glc), 2, petunidin-3-glucoside (Pt3glc), 3, peonidin-3-glucoside (Pn3glc) (Figure I.A). The blackberry anthocyanin rich extract was analysed and four anthocyanins were identified: 5, cyanidin-3-glucoside (Cy3glc), 6, cyanidin-3-rutinoside (Cy3rut), 7, cyanidin-3-dioxaloyl-glucoside (Cy3dioxaglc), and 8, cyanidin-3-malonyl-glucoside (Cy3manglc) (Figure I.B). Purification of Mv3glc and Cy3glc from each extract was evaluated by HPLC and a degree of purity of 85.44 % and of 98.30 %, respectively, was estimated (Figure I.C and D).

3.1 Cytotoxic Effect of Anthocyanins Towards Keratinocytes

3.1.1 Traditional Method

The effect of anthocyanin extracts (red wine and blackberry extract) and of their major anthocyanins (Mv3glc and Cy3glc, respectively) on keratinocytes cytotoxicity was assayed by traditional and real-time impedance methods.

Briefly, in the colorimetric assay human keratinocytes were exposed to a serial range of concentrations (from 6.25 to 100.0 μM) of each compound or extract, for 48 h during the log phase (Figure II). These extracts and their major pigments showed no cytotoxicity up to the highest concentration of 100.0 μM, except for blackberry anthocyanin extract that presented significant differences from control for the maximal concentration tested. Inhibition rate was of approximately 27 % and this may be caused by the presence of other cyanidin derivatives that may influence proliferation for this cell line. On the other hand, it is possible that this antiproliferative activity may be a result of a synergistic effect between the species present in the extract. Considering the possible application of these compounds in cosmetic formulations, the following tests were performed at the concentration of 20 μM quite bellow the maximal concentration used of an active compound in formulations (< 1 %). An example of this is reported for grape fruit extract in the literature [5], stating that for most products a concentration of 0.4 to 0.5 % is usually used. It should be further noticed that these are all *in vitro* assays with a single type cells monolayer. Assays exploring the effect of compounds in more complex skin systems may probably need greater concentrations to be used. Bearing this, the concentration of 20 μM was validated for the following studies, as all tested

View Article Online
DOI: 10.1039/C7FO01239J

compounds showed no antiproliferative effect on keratinocytes at this concentrations, which validates the execution of wound-healing assays.

3.1.2 Real-Time Cellular Impedance Method

For the real-time method, a model for keratinocyte cells monolayer was optimized using ECIS, studying the effect of cellular density at inoculation time. Figure III shows the resistive portion of impedance normalized to its value at the start of each run, at 4 kHz, for the two cellular densities tested: 1.6×10^5 or 1.6×10^6 cells/mL. As the cell attach and spread on the surface of the electrode, resistance increases, as the passage of current at this frequency is constrained by the insulating membranes of the cells. However, there is a significant difference between the two different densities. While cells inoculated at 1.6×10^5 cells/mL take up more than 50 hours to reach confluency and with no reproducibility amongst wells, when HaCat cells are inoculated at 1.6×10^6 cells/mL, the time at which the confluent monolayer is established is shortened to 10 hours (Figure III.A and B) and all wells present a similar behaviour. When confluency is reached, resistance fluctuates slightly with time, due to the micro-movements in the cell monolayer, considered to be an indicative of living cells.

The time course of the measured capacitance gives further insight to the attachment and spreading of cells into the microelectrode. To characterize the spreading of HaCat cells on the electrodes, coated with 1% gelatin, two different measures were calculated from the time courses: the $t_{1/2}$, which is the time necessary to produce a half-maximum drop in capacitance, corresponding to the time cells need to spread out on half of the electrode area; and the average slope of the capacitance shift between 1 and 6 nF, by means of linear regression, which corresponds to the rate of spreading. These measures are shown in figure IV (graphical exemplification of one well) and were calculated from 8 independent wells inoculated with 1.6×10^6 cells/mL. The half time was calculated to be approximately 3.55 ± 0.67 hours, and the rate of spreading, in these conditions, to be of 0.44 ± 0.03 nF per hour.

A control was performed with several concentrations of DMSO (0.01-10 %) to validate cytotoxicity assays performed using ECIS. DMSO was chosen since it is the solvent in which all the stock solutions were prepared and because different studies report DMSO cytotoxicity towards different cell lines [19, 20].

The effect of 4 different DMSO concentrations on the overall resistance of the HaCat cell monolayer was monitored for 24 h. Sixteen electrodes were followed one after

View Article Online
DOI: 10.1039/C7FO01239J

another with each well's data point requiring a few seconds. Data is presented as the measured resistance normalized to its value at the beginning of each run (Figure V). A drastic drop of resistance is observed almost immediately for the concentrations of 5 and 10 %. The concentrations of 0.01 % and 1 % seem to have no significant effect on resistance. To further understand DMSO cytotoxicity, two strategies were employed. Frequency scan measurements were taken after 24 h exposure to the three different DMSO concentrations tested and to analyse the differences in resistance curves, values were normalized by dividing the values of cell covered electrodes by those of a cell-free electrode, as explored in the literature [13] (Figure V). A peak is observed at 4 kHz for the control, which was expected for cell-covered electrode, as explored in the literature [13] and experimentally explored (data not shown). This peak in normalized resistance seems to be maintained for 0.01 and 1 % and disappears with the increasing concentration of DMSO, demonstrating that for these concentrations resistance values converge to those of a cell-free electrode (Figure VI).

Further, data was modelled as described elsewhere [9], which allowed the calculation of R_b and α parameters, measures of cell-cell and cell-matrix interactions, respectively and Cm, a measure of cell membrane integrity. The results are presented in Table I. Notice that the fitting could only be applied to data from the control wells and up to 1 % DMSO, once the two other concentrations of DMSO caused damage to the cell monolayer and, so, the model cannot be used when cells are not confluent. There is no significant difference between the values of Rb, α and Cm, as statistically analysed by one-way ANOVA, followed Bonferroni test, which indicates that up to 1% DMSO there is no damage to the monolayer function, neither to the interactions between cells and the gelatin matrix or even to the integrity of the cellular membrane.

After analysing the results for the positive control, cytotoxicity assays were performed for the anthocyanin extracts and their major purified pigments (final DMSO concentration = 0.01 %). Figure VII represents an example of data obtained during these experiments as a typical graph of resistance normalized to its value exactly before compound addition vs time. Incubation was carried over 24 h and compounds seem to have no effect on resistance values over time. Thereafter, and to further understand the effect of anthocyanins on HaCat cells integrity, data was modelled as before for the positive control. Rb, α and Cm parameters were calculated with ECIS software and are presented on Table II. There were no statistical differences observed for any of the compounds at the tested concentration (20 μM). This complemented the results obtained

View Article Online
DOI: 10.1039/C7FO01239J

with the SRB assay, stating that red wine and blackberry anthocyanin extract, as well as their major anthocyanins (Mv3glc and Cy3glc) showed no effect on HaCat cell proliferation, up to 100 μM.

It is of notice that the values obtained for these parameters were not similar to the literature [21] for this cell line. The values of Rb and α were around 2.40, while the literature states Rb value to be around 1.2 Ω cm^2 and α of around 5 $\Omega^{0.5}$cm. Finally, C_m is described to be of 2 μF/cm^2 and, in the conditions applied in these studies, it was calculated to be of 2.80 μF/cm^2, approximately. This may be due to the different conditions used prior to cell seeding, once we cover the electrodes with gelatin before seeding and let grow for 24 hours and then incubated with medium or compounds for more 24 hours. In the literature, parameters were calculated 12 hours after cells reached confluence. These modifications may contribute to the differences observed in the data obtained for the three parameters.

3.1.3 The effect of anthocyanins on micromotion

To better understand the effect of anthocyanins on keratinocytes, micromotion measurements were performed on HaCat cell monolayer, 24 h after exposure to the compounds, when the cultures did not exhibit a large fluctuation in the measured impedance, but presented a sort of noise that could be analysed if measures were taken faster. The measurements were then taken at 4 kHz AC signal and the fluctuations in the resistance were analysed first by plotting resistance data normalized to the average resistance for the whole period (Figure VIII). In this case, neither the anthocyanin extracts nor the purified compounds showed a drastic deviation from control wells.

Furthermore, these fluctuations were mathematically analysed using three numerical methods: the fast Fourier transform (FFT), variance and variance of increment [11, 13]. Results are shown in Table III and expressed as a single number as the average resistance for the whole period of 2048-s, the slope of the log-log plot of power spectrum, the variance for the 32-point intervals (Var32) and the variance of increments for the 32-point sampling intervals (Voi32) of the normalized 2048-s data set. The power slope was estimated with the least-square straight-line fit of power at the lowest 100 frequencies (excluding the first and the last). The Var32 was obtained by calculating the statistical variance for each 32-point segment of the 2048-point data and then taking the average of these 64 points. The Voi32 was calculated as the variance of the increments between the 32-point sampling intervals, considering that the data was

View Article Online
DOI: 10.1039/C7FO01239J

sampled every 32 s, and then taking the 64 data points and calculating the 63 increments.

Taking all the calculated parameters, it is possible to conclude that anthocyanin extracts and the isolated compounds showed no cytotoxicity for HaCat cells. There was no statistical evidence that the tested pigments compromise the micromovements of a keratinocyte monolayer, which complements the data obtained from the modelling of impedance values, where no difference was observed for all three parameters. This is relevant for the validation of compound usage in formulations, once it is desirable that the compounds present no cytotoxicity towards skin cells, and further validating the implementation of assays testing the potential beneficial activities of the compounds.

3.2 Wound Healing Assay

Wound-healing assays are of importance when considering skin-care, because the skin is the primary barrier towards any external assault such as mechanical wounding. ECIS was used to evaluate the effect of anthocyanins in healing process of a damaged keratinocyte monolayer. This system has a great advantage when compared to traditional wound assays such as the scratch assay. As wounding is through an electrical signal, the assay is reproducible because the wound is always performed in the exact same way. On the other hand, the healing progress is monitored in real-time and results can be easily evaluated either by resistance or capacitance measures.

The electrical wound was applied after pre-incubation with compounds for 24 h using an higher frequency (60000 Hz) and current (2400 μA) capable of wounding the cell monolayer, and resulting in an abrupt drop in impedance to values like those of a free-cell well. Thereafter, cells around the microelectrode started to migrate and proliferate from the surroundings towards the microelectrode surface. Figure IX.A shows the data for the resistive part of impedance versus time, in this graph it is clear the positive influence of anthocyanin rich extracts and their major anthocyanins in wound recovery. Indeed, the time cells take to migrate and proliferate is shortened when in the presence of anthocyanins. This behaviour was quantified as the difference in resistance at different times after wounding (Figure IX.B). Significant differences were found 5 hours after the electrical wound, for the Cy3glc and blackberry anthocyanin extract. In the case of Mv3glc, there is also a significant difference in resistance for Mv3glc, 10 hours after. After this time, resistance values from compounds and extracts

View Article Online
DOI: 10.1039/C7FO01239J

reach a plateau, and the same happens with control, meaning that, at 15 hours after wounding, all wells are confluent again and monolayer function is restored.

On the other hand, recovery from wounding can also be analysed considering the capacitive part of impedance. Figure X. A represents these measures over time where it is possible to observe the positive effect of compounds in the wound recovery. The time at 50 % recovery was calculated from this representation modelling the values of capacitance as a % of the initial values immediately after the wound. Significant statistical differences were found for both extracts and their major isolated anthocyanins as shown in Figure X.B. While control wells take 4.91 (± 1.11) hours to recover 50 % of the damage, Cy3glc showed the best results, taking up to 1.48 (± 0.15) hours, followed by blackberry extract with 2.01 (± 0.18) hours. On the other hand, cells recover 50 % of the injury in 2.03 (± 0.09) hours with Mv3glc and 2.36 (± 0.76) when exposed to red wine anthocyanin extract. These results indicate that anthocyanins interfere with wound recovery in a keratinocyte cell monolayer, which may indicate that these polyphenols may positively modulate the cicatrisation of skin. The fact that the more complex extracts tested maintain the positive effect showed for the purified compounds is of major interest when thinking about industrial application, where more abundant and easily obtained ingredients are crucial for scaling up stage and commercialization process.

These results confirm those found in the literature [22], for anthocyanins extracted from black soybean, composed of Cy3glc (the major), but also of Dp3glc and Pt3glc (also present in red wine anthocyanin extract) that potentiated wound healing in a scratch wound assay. Taken together, anthocyanins from red wine and from blackberry, particularly Mv3glc and Cy3glc, respectively, might be potential ingredients for cosmetic formulations to effectively help in the treatment of possible wounding that are probable to occur as skin is the most external organ, but more studies must be performed taking into consideration the presence of the other cellular types that make up skin and the environment into which they are networking. On the other hand, it is also possible to conclude that ECIS has indeed several advantages when compared to other traditional methods. In fact, ECIS allows the screening of compounds cytotoxicity considering both the effect of compounds on cell-cell as well as to cell-matrix interactions, by calculating Rb and α parameters through the ECIS model. Furthermore, ECIS wound-healing assay allows the execution of reproducible assays as it is based on electrical wound and real-time monitoring of impedance.

View Article Online
DOI: 10.1039/C7FO01239J

4. ACKNOWLEDGEMENTS

This research was supported by a research project grant (PTDC/AGR-TEC/3078/2014) with financial support from FCT/MEC through national funds and co-financed by FEDER, under the Partnership Agreement PT2020 (UID/QUI/50006/2013 – POCI/01/0145/ FEDER/007265). Iva Fernandes gratefully acknowledges the Post-Doctoral Grant from FCT (SFRH/BPD/86173/2012).

View Article Online
DOI: 10.1039/C7FO01239J

5. REFERENCES

1. L. M. Soto, E. Falqué and H. Domínguez, Relevance of Natural Phenolics from Grape and Derivative Products in the Formulation of Cosmetics, *Cosmetics*, 2015, **2**.
2. L. Nan, O. Kehui, C. Jiaoying, Y. Wuying and W. Wenjun, Research on Anti-oxidant Activity and Hypolipemic Mechanism of Aloes Flavonoids in Mice, *Food Nutr. Res.*, 2014, **2**, 601-607.
3. D. Li, P. Wang, Y. Luo, M. Zhao and F. Chen, Health benefits of anthocyanins and molecular mechanisms: Update from recent decade, *Crit. Rev. Food Sci. Nutr.*, 2017, **57**, 1729-1741.
4. J. A.-A. Shipp, El-Sayed M. , Food Applications and Physiological Effects of Anthocyanins as Functional Food Ingredients *Open Food Sci. J.*, 2010, **4**, 7-22.
5. M. Soto, E. Falqué and H. Domínguez, Relevance of Natural Phenolics from Grape and Derivative Products in the Formulation of Cosmetics, *Cosmetics*, 2015, **2**, 259.
6. Y. Cui, Y. An, T. Jin, F. Zhang and P. He, Real-time monitoring of skin wound healing on nano-grooves topography using electric cell-substrate impedance sensing (ECIS), *Sens. Actuators B Chem.*, 2017, **250**, 461-468.
7. Y. Koo and Y. Yun, Effects of polydeoxyribonucleotides (PDRN) on wound healing: Electric cell-substrate impedance sensing (ECIS), *Mater. Sci. Eng. C*, 2016, **69**, 554-560.
8. R. Szulcek, H. J. Bogaard and G. P. van Nieuw Amerongen, Electric Cell-substrate Impedance Sensing for the Quantification of Endothelial Proliferation, Barrier Function, and Motility, *J. Vis. Exp.*, 2014, **28**, e51300.
9. I. Giaever and C. R. Keese, Micromotion of mammalian cells measured electrically, *Proc. Natl. Acad. Sci. U. S. A.*, 1991, **88**, 7896-7900.
10. M. Y. Lee, A. Skoura, E. J. Park, S. Landskroner-Eiger, L. Jozsef, A. K. Luciano, T. Murata, S. Pasula, Y. Dong, M. Bouaouina, D. A. Calderwood, S. M. Ferguson, P. De Camilli and W. C. Sessa, Dynamin 2 regulation of integrin endocytosis, but not VEGF signaling, is crucial for developmental angiogenesis, *Development*, 2014, **141**, 1465.
11. C.-M. Lo, C. R. Keese and I. Giaever, Monitoring Motion of Confluent Cells in Tissue Culture, *Exp. Cell Res.*, 1993, **204**, 102-109.
12. V. Bondu, R. Schrader, A. M. Gawinowicz, P. McGuire, A. D. Lawrence, B. Hjelle and T. Buranda, Elevated Cytokines, Thrombin and PAI-1 in Severe HCPS Patients Due to Sin Nombre Virus, *Viruses*, 2015, **7**.
13. D. Opp, B. Wafula, J. Lim, E. Huang, J.-C. Lo and C.-M. Lo, Use of electric cell-substrate impedance sensing to assess in vitro cytotoxicity, *Biosens. Bioelectron.*, 2009, **24**, 2625-2629.
14. C. E. Campbell, M. M. Laane, E. Haugarvoll and I. Giaever, Monitoring viral-induced cell death using electric cell–substrate impedance sensing, *Biosens. Bioelectron.*, 2007, **23**, 536-542.
15. T. B. Tran, S. Cho and J. Min, Hydrogel-based diffusion chip with Electric Cell-substrate Impedance Sensing (ECIS) integration for cell viability assay and drug toxicity screening, *Biosens. Bioelectron.*, 2013, **50**, 453-459.
16. C. R. Keese, J. Wegener, S. R. Walker and I. Giaever, Electrical wound-healing assay for cells in vitro, *Proc. Natl. Acad. Sci. U. S. A.*, 2004, **101**, 1554-1559.
17. L. Cruz, I. Fernandes, M. Guimaraes, V. de Freitas and N. Mateus, Enzymatic synthesis, structural characterization and antioxidant capacity assessment of a new lipophilic malvidin-3-glucoside-oleic acid conjugate, *Food Funct.*, 2016, **7**, 2754-2762.
18. C. F. Marques, Iva; Norberto, Sónia; Sá, Carla; Teixeira, Diana; De Freitas, Victor; Mateus; Calhau, Conceição; Faria, Ana, Pharmacokinetics of blackberry anthocyanins consumed with or without ethanol: a randomized and crossover trial, *Mol. Nutr. Food Res.*, 2016, DOI: 10.1002/mnfr.201600143.

View Article Online
DOI: 10.1039/C7FO01239J

19. T. I. Malinin and V. P. Perry, Toxicity of dimethyl sulfoxide on HeLa cells, *Cryobiology*, 1967, **4**, 90-96.
20. G. Da Violante, N. Zerrouk, I. Richard, G. Provot, eacute, rard, J. C. Chaumeil and P. Arnaud, Evaluation of the Cytotoxicity Effect of Dimethyl Sulfoxide (DMSO) on Caco2/TC7 Colon Tumor Cell Cultures, *Biol. Pharm. Bull.*, 2002, **25**, 1600-1603.
21. S.-E. Chow, C. P.-C. Chen, C.-C. Hsu, W.-C. Tsai, J.-S. Wang and N.-C. Hsu, Quantifying cell behaviors in negative-pressure induced monolayer cell movement, *Biomed. J.*, 2016, **39**, 50-59.
22. I. T. Nizamutdinova, Y. M. Kim, J. I. Chung, S. C. Shin, Y.-K. Jeong, H. G. Seo, J. H. Lee, K. C. Chang and H. J. Kim, Anthocyanins from black soybean seed coats stimulate wound healing in fibroblasts and keratinocytes and prevent inflammation in endothelial cells, *Food Chem. Toxicol.*, 2009, **47**, 2806-2812.

View Article Online
DOI: 10.1039/C7FO01239J

Table I. ECIS parameters calculated for HaCat monolayer after 24 h exposure to DMSO.

% DMSO	Rb (Ω cm^2)	α ($\Omega^{0.5}$cm)	Cm (μF/cm^2)
0	2.23 ± 0.50	2.25 ± 0.14	2.48 ± 0.06
0.01	2.41 ± 0.04	2.41 ± 0.13	2.78 ± 0.14
1	2.22 ± 0.45	2.24 ± 0.37	2.46 ± 0.10

Table II. ECIS parameters calculated for HaCat monolayer after 24 h exposure to the anthocyanin extracts and the purified anthocyanins at 20 µM. There was no statistically significant difference.

Compound	Rb (Ω cm^2)	α ($\Omega^{0.5}$cm)	Cm (μF/cm^2)
Control	2.41 ± 0.04	2.41 ± 0.13	2.78 ± 0.14
Mv3glc	2.46 ± 0.09	2.59 ± 0.11	2.60 ± 0.06
Red wine extract	2.21 ± 0.29	2.25 ± 0.22	2.75 ± 0.13
Cy3glc	2.22 ± 0.06	2.24 ± 0.05	2.81 ± 0.06
Blackberry extract	2.29 ± 0.08	2.57 ± 0.12	2.55 ± 0.05

Table III. ECIS micromotion data obtained from confluent HaCat layers 24h after exposure to purified anthocyanins and their extracts at 20 µM. The column labeled Resistance is the average resistance value of the cell layer over a 2048-s run. The column labeled power slope is the slope of the log–log plot of power versus frequency. The column labeled Var32 is the statistical variance for the 32-point intervals of the normalized 2048-s data set. The column labeled VoI32 is the variance of the increments for the 32-point sampling intervals of the 2048-s data set. The column labeled Hurst is the Hurst exponent. Values shown are mean ± standard error (n = 4-7 for each compound).

Compound	Resistance (kΩ)	Power slope	Var32 (10^{-7})	VoI32 (10^{-6})	Hurst
Control	9.11 ± 0.46	2.14 ± 0.10	3.24 ± 0.63	1.190 ± 0.007	0.870 ± 0.123
Mv3glc	10.24 ± 0.84	2.22 ± 0.14	5.68 ± 1.40	1.310 ± 0.003	0.997 ± 0.002
Red wine extract	8.36 ± 0.49	2.06 ± 0.13	2.39 ± 0.36	1.140 ± 0.008	1.001 ± 0.002
Cy3glc	9.10 ± 0.30	2.07 ± 0.19	2.32 ± 0.65	1.260 ± 0.005	0.997 ± 0.003
Blackberry extract	9.72 ± 0.12	2.08 ± 0.13	2.80 ± 0.66	1.340 ± 0.002	1.001 ± 0.001

View Article Online
DOI: 10.1039/C7FO01239J

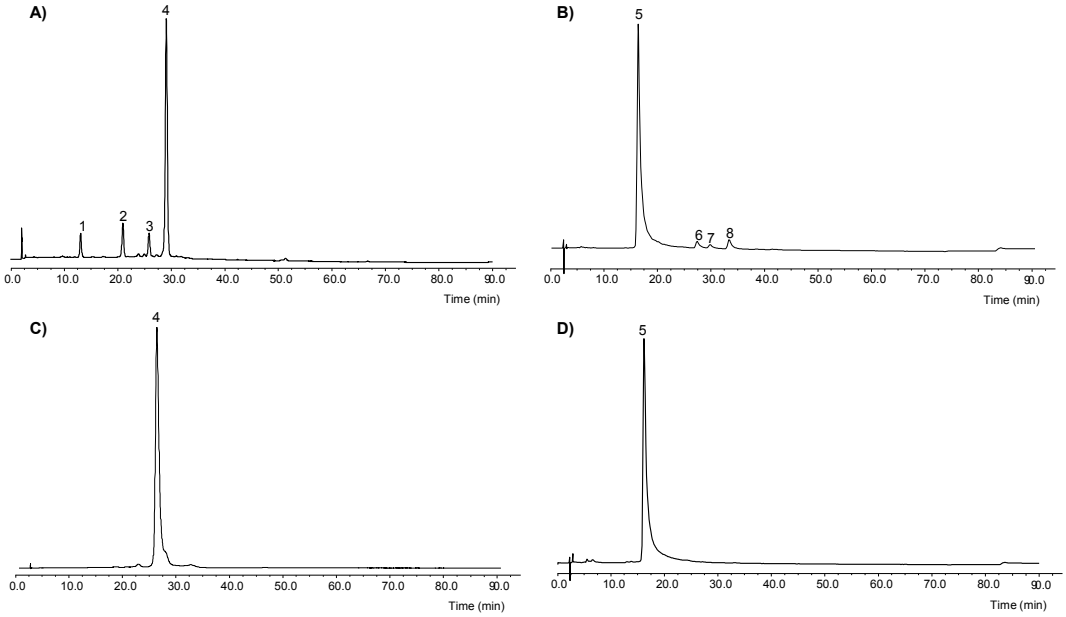

Figure I. Representative HPLC chromatograms of isolated anthocyanins from wine (A) and its major anthocyanin, Mv3glc (C) and a blackberry anthocyanin extract (B) and its major anthocyanin, Cy3glc (D) obtained from blackberry anthocyanin extract. 1) Dp3glc: delphinidin-3-O-glucoside; 2) Pt3glc: petunidin-3-O-glucoside; 3) Pn3glc: peonidin-3-O-glucoside; 4) Mv3glc: malvidin-3-O-glucoside; 5) Cy3glc: Cyanidin-3-O-glucoside; 6) Cy3rut: Cyanidin-3-rutinoside, 7) Cy3dioxaglc: Cyanidin-3-dioxaloyl-glucoside and 8) Cy3manglc: Cyanidin-3-malonyl-glucoside.

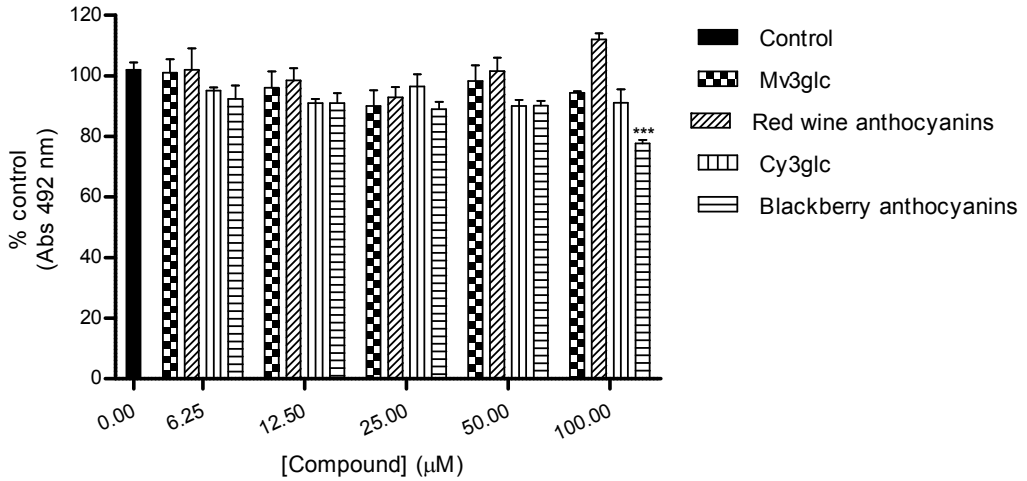

Figure II. Effect of anthocyanin extracts and purified anthocyanins Mv3glc and Cy3glc, on HaCat cells proliferation evaluated by SRB assay. HaCat cells, seeded in 96 well plates, were treated with a concentration range (6.25 – 100.00 μM) of each

View Article Online
DOI: 10.1039/C7FO01239J

compound for 48 h. Each value represents the mean ± SEM (n=6) ***p < 0.001 (significant decrease vs control).

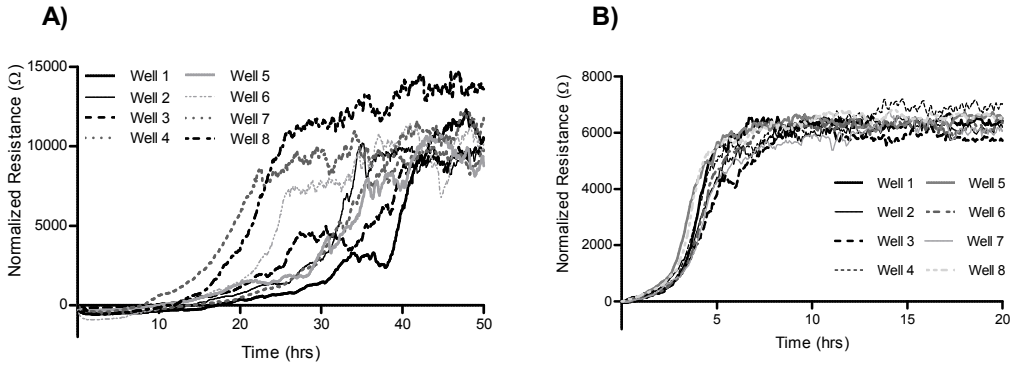

Figure III. Graphs A and B represent a single eight-well array (8W1E) seeded with 1.6 × 10^5 cell/ml or 1.6 × 10^6 cell/ml, respectively, using DMEM-F12 medium. Resistance values were measured at 4 kHz and normalized according to the basal values ($R_n - R_0$).

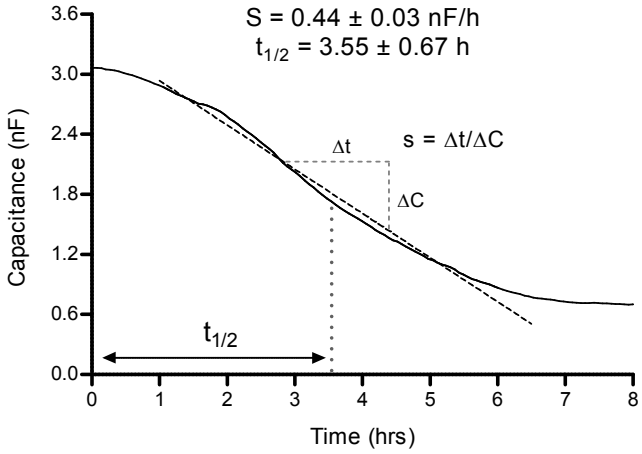

Figure IV. Representative graph of one well time course of the capacitance measured at 64 kHz when HaCat cells are seeded into ECIS arrays at 1.6 × 10^6 cell/ml. Two measures were calculated from this data characterizing the spreading of HaCat cells on gelatin coated gold microelectrodes. $T_{1/2}$ denotes the time necessary to achieve half-maximum capacitance drop. Cell spreading rate was also calculated as the slope of the linear regression between C = 1.0 nF and C = 6.0 nF. The data from 8 individual wells were used to calculate these values.

View Article Online
DOI: 10.1039/C7FO01239J

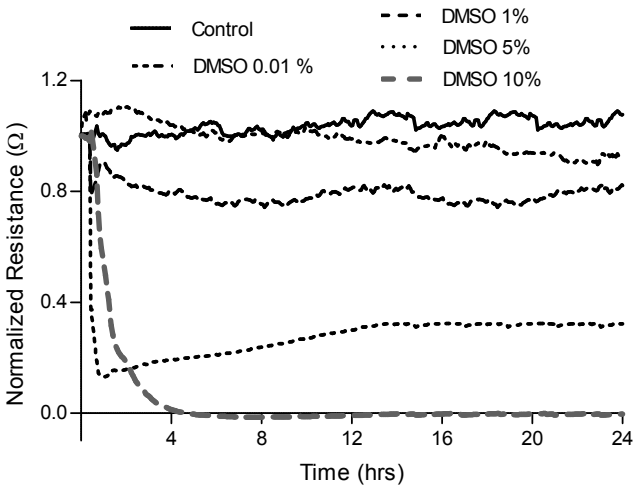

Figure V. Graph represents a positive control performed with DMSO to validate cytotoxicity assays. Resistance values were normalized to the value of resistance exactly before the addition of compounds ($\frac{R_n}{R_0}$). Four different concentrations (0.01, 1, 5 and 10 % of DMSO in DMEM-F12 medium) were tested in HaCat cell monolayer over 24 h incubation.

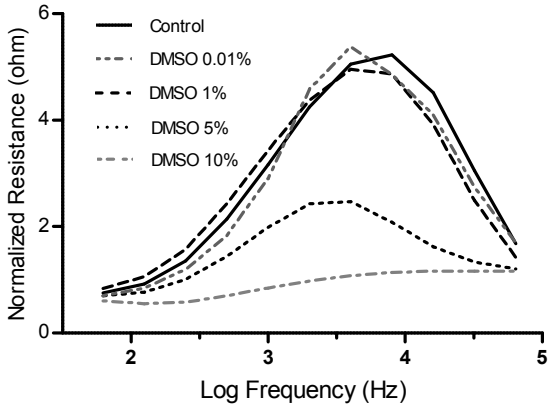

Figure VI. Graph represents normalized resistance $\left(\frac{R_n}{R_{Free-cell\ well}}\right)$ as a function of the Log (frequency) obtained after 24 h of incubation of cells with different DMSO concentrations.

View Article Online
DOI: 10.1039/C7FO01239J

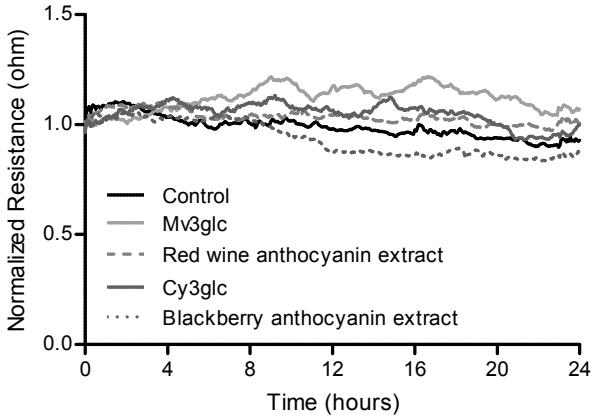

577

578 **Figure VII.** Graph represents an example of data obtained from cytotoxicity assays
579 with red wine and blackberry anthocyanin extracts as well as purified Mv3glc and
580 Cy3glc. Resistance values were normalized to the value of resistance exactly before the
581 addition of compounds ($\frac{R_n}{R_0}$).

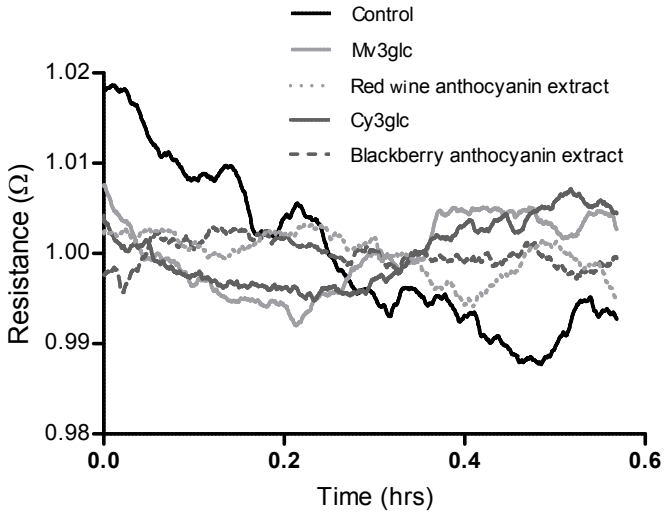

582

583 **Figure VIII.** Normalized resistance data ($\frac{R_n}{R_{average\ of\ whole\ period}}$) recorded after 24 h of
584 incubation of a confluent HaCat cell layer with compounds or with medium alone.
585

View Article Online
DOI: 10.1039/C7FO01239J

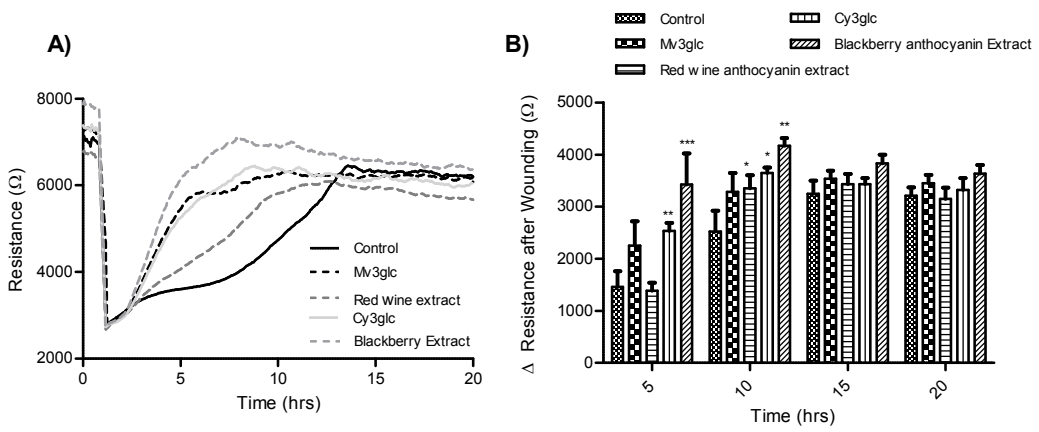

Figure IX. Wound-healing assay for HaCat cells using ECIS. A) ECIS real-time resistance after wounding in response to red wine and blackberry anthocyanin extracts as well as to Mv3glc and Cy3glc, at the concentration of 20 µM. B) Graph of difference in resistance at several time points after wounding. Each value represents the mean ± SEM (n=4-5) *p < 0.05, **p < 0.01, ***p < 0.001 (significant increase vs control).

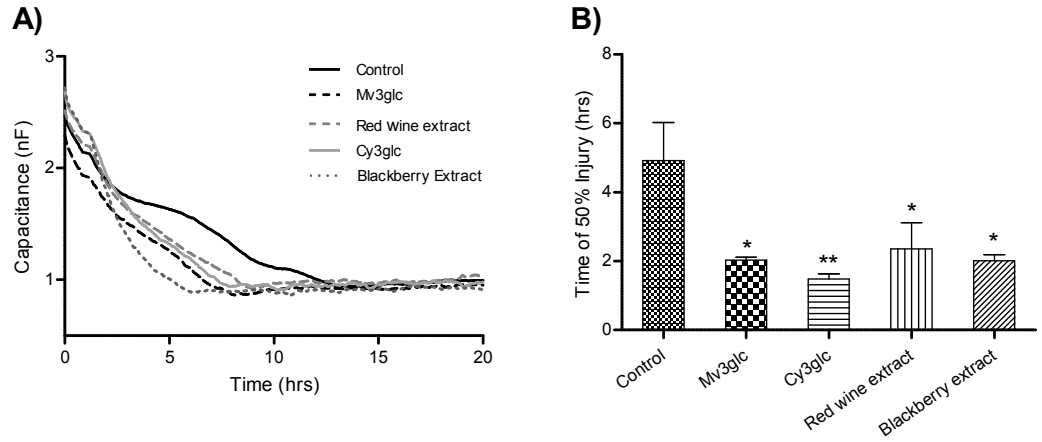

Figure X. Wound-healing assay for HaCat cells using ECIS. A) ECIS real-time capacitance after wounding (time 0 hours) in response to red wine and blackberry anthocyanin extracts as well as to Mv3glc and Cy3glc, at the concentration of 20 µM. B) Time needed for cells to recover 50 % from the injury caused at wound in the presence of DMEM-F12 medium (Control) or in the presence of anthocyanin extracts and purified anthocyanins. Each value represents the mean ± SEM (n=4-5) *p < 0.05, **p < 0.01 (significant decrease vs control).

View Article Online
DOI: 10.1039/C7FO01239J

Table of content

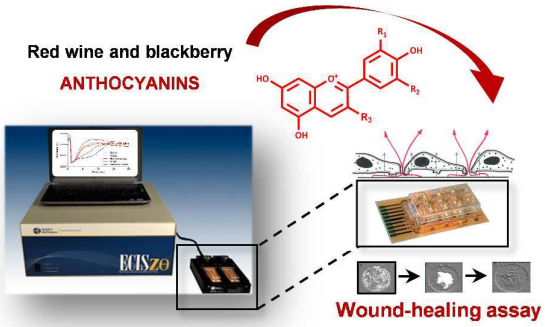

Anthocyanins enhanced the healing rate of keratinocyte cells